Carbohydrate Research 354 (2012) 32–39

Contents lists available at SciVerse ScienceDirect

Carbohydrate Research

journal homepage: www.elsevier.com/locate/carres

Research on the structure–surface adsorptive activity relationships of triazolyl glycolipid derivatives for mild steel in HCl

Hai-Lin Zhang, Xiao-Peng He *, Qiong Deng, Yi-Tao Long, Guo-Rong Chen *, Kaixian Chen

Key Laboratory for Advanced Materials & Institute of Fine Chemicals, East China University of Science and Technology, 130 Meilong Road, Shanghai 200237, PR China

ARTICLE INFO

Article history:
Received 4 February 2012
Received in revised form 6 March 2012
Accepted 7 March 2012
Available online 17 March 2012

Keywords:
Glycolipid
Cue-AAC
EIS
Corrosion
Inhibitor

ABSTRACT

Triazolyl glycolipid derivatives constructed via Cu^{I}-catalyzed azide-alkyne 1,3-dipolar cycloaddition reaction (Cue-AAC) represent a new range of carbohydrate-based scaffolds for use in many fields of the chemical research. Here the surface adsorptive ability of series of our previously prepared C1- or C6-triazole linked gluco- and galactolipid derivatives for mild steel in 1 M HCl was studied via electrochemical impedance spectroscopy (EIS). Results indicated that these monosaccharide–fatty acid conjugates are weak inhibitors against HCl corrosion for mild steel. Moreover, some newly synthesized triazolyl disaccharide (maltose)–fatty alcohol conjugates failed to display enhanced activity, meaning that the structural enlargement of the sugar moiety does not favor the iron surface adsorption. However, a bis-triazolyl glycolipid derivative, which was realized by introducing a benzenesulfonamide group via Cue-AAC to the C6-position of a C1-triazolyl glucolipid analog, eventually showed significantly improved adsorptive potency compared to that of its former counterparts. The corrosion inhibitive modality of this compound for mild steel in HCl was subsequently studied via potentiodynamic polarization and thermodynamic calculations.

1. Introduction

During the everyday industrial washing and scaling processes of various metallic equipments in acidic solutions, the presence of corrosion inhibitors may necessarily assuage the excessive dissolution of heavy metals that harm both nature and our health. Due to their structural versatility, easy accessibility and superior potency, organic compounds are now frequently used in place of inorganic materials for corrosion inhibition. However, despite the good protective ability of the numerous identified small-molecule corrosion inhibitors for metals, the toxic nature of these compounds embodying extensive polycyclic rings yet lowers their potential toward industrialization.[1] As a result, identification of environmentally friendly corrosion inhibitors that simultaneously possess admirable inhibitive potency becomes the mainstream of current corrosion investigations.

Some natural products including amino acids and plant extracts have been proposed, alternatively, as the green surrogates of present corrosion inhibitors.[2–5] Nevertheless, they also have limitations that hamper the further commercialization. On the one hand, isolation of products from natural resources may be of low efficiency due to the long extraction time/step and poor isolated yields. On the other hand, despite their abundance in nature, most of the structurally simple amino acids lack essentially the potency for metal surface adsorption. Therefore, the exertion of efficient chemical modifications upon easily available natural metabolites could become a promising strategy for acquiring potency-enhanced corrosion inhibitors with potentially retained greenness.

Taking nature's hint for the creation of her primary metabolites such as polysaccharides, polynucleosides, and polypeptides, Sharpless and co-workers coined 'Click Chemistry' a decade ago.[6] This new synthetic concept prompts the exploration of efficient carbon-heteroatom ligation reactions for the modular construction of useful compound libraries in high yields without tedious laboratorial workup. Cu^{I}-catalyzed azide-alkyne 1,3-dipolar cycloaddition reaction (Cue-AAC)[7–9] in forming the unique 1,4-disubstituted 1,2,3-triazoles represents arguably the best paradigm of click chemistry, and has realized the effective construction of myriad functional compounds including triazole-functionalized carbohydrate derivatives.[10–23]

Enlightened by this, we sought to synthesize triazole-modified natural products as our strategy for the innovation of new corrosion inhibitors. Since the sugar moiety in connection with a triazole group is envisioned capable for metal surface adsorption, while their lipid end could form presumably additional protective films by generating lipid arrays over the surface, we report here a research on the structure–surface adsorption activity relationships of triazolyl glycolipids for mild steel in HCl. The adsorptive ability

* Corresponding authors. Tel.: +86 21 64253016; fax: +86 21 64252758.
E-mail addresses: xphe@ecust.edu.cn (X.-P. He), mrs_guorongchen@ecust.edu.cn (G.-R. Chen).

0008-6215/$ - see front matter © 2012 Elsevier Ltd. All rights reserved.
http://dx.doi.org/10.1016/j.carres.2012.03.006

of three series of our previously synthesized triazolyl monosaccharide–fatty acid conjugates was first tested for mild steel in HCl via electrochemical impedance spectroscopy (EIS).

2. Results and discussion

Preparation of triazole-functionalized glycolipid derivatives has been reported by several independent research groups.[24–28] These new carbohydrate–lipid conjugates have addressed interesting properties through many interdisciplinary studies.

Recently, we have disclosed three series of novel C1- or C6-triazole-linked monosaccharide–lipid conjugates constructed via Cue-AAC, shown in Figure 1.[26–28] A preliminary EIS study indicated that the C1-substituted glycolipids **1–9** have good ability for gold surface adsorption in CH_2Cl_2.[26] As a result, we chose to measure practically the surface adsorptive potency of these compounds, and that of their C6-triazole-linked gluco- and galactolipid analogues for the industrially frequently used mild steel in 1 M HCl via EIS.

A conventional three-electrode assembly that comprises the mild steel with 1.0 cm^2 exposed surface area as the working electrode, platinum foil as the counter electrode, and a saturated calomel electrode (SCE) as the reference electrode, was used for electrochemical experiments. The electrochemical process of these electrodes in the absence and presence of compounds **1–27** (10^{-3} M) in 1 M HCl was examined via EIS at open-circuit potential and the resulting Nyquist plots are given in Figure S-1.

According to the suited equivalent circuit model for these plots (Fig. 7, Section 4), the corresponding impedance parameters including solution resistance (R_s), charge transfer resistance (R_{ct}), constant phase element (CPE) and phase shift (n) were obtained and the inhibitive efficiencies (η) were calculated (Table 1), in which CPE is frequently used in place of a double layer capacitance

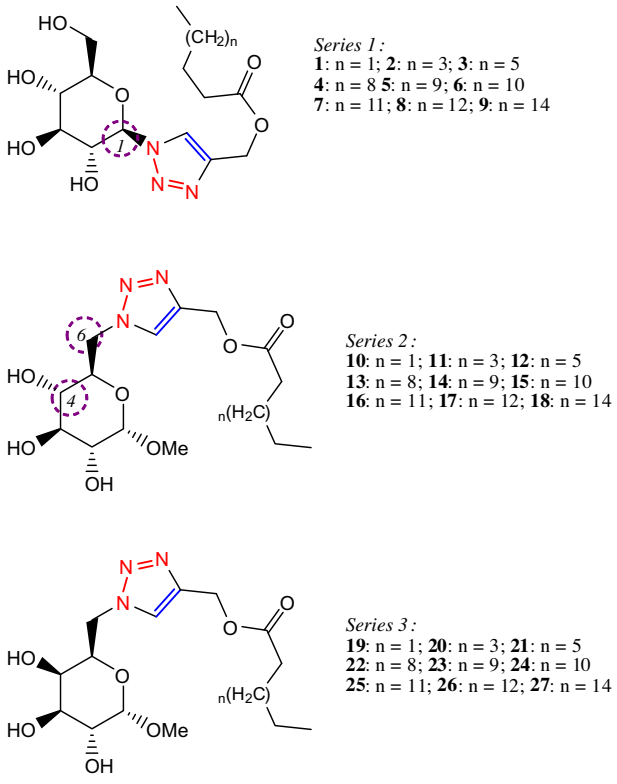

Figure 1. Previously synthesized C1- or C6-substituted triazolyl glycolipid derivatives.

Table 1
EIS parameters for mild steel in 1 M HCl without (blank) and with compounds **1–27**

Compd	R_s (Ω cm^2)	R_{ct} (Ω cm^2)	CPE (μF cm^{-2})	n	η (%)
Blank	4.19	62.72	295.7	0.80	n.a.[a]
1	8.05	77.33	127.0	0.82	18.9
2	6.89	87.03	129.4	0.83	27.9
3	5.96	83.78	119.9	0.84	25.1
4	10.68	105.2	106.4	0.82	40.4
5	7.50	109.8	108.5	0.83	42.9
6	5.97	106.2	122.3	0.83	40.9
7	10.71	112.0	107.6	0.82	44.0
8	7.58	114.8	188.7	0.83	45.4
9	10.05	105.3	154.3	0.79	40.4
10	9.22	99.57	91.12	0.83	37.0
11	6.84	88.99	301.6	0.79	29.5
12	10.68	103.0	106.4	0.82	39.1
13	10.76	131.9	121.6	0.80	52.4
14	10.73	123.1	128.1	0.80	49.0
15	4.16	120.9	300.7	0.78	48.1
16	6.58	113.3	107.3	0.83	44.6
17	5.22	113.5	100.7	0.84	44.7
18	5.88	118.7	102.8	0.83	47.2
19	8.12	66.88	148.4	0.81	6.22
20	9.80	77.94	157.4	0.79	19.5
21	5.85	73.62	290.5	0.79	14.8
22	5.39	79.58	255.5	0.80	21.2
23	4.20	127.8	92.04	0.84	50.9
24	9.90	103.7	129.0	0.80	39.5
25	7.28	103.9	103.2	0.83	39.6
26	4.24	105.9	102.1	0.83	40.8
27	10.74	104.1	106.0	0.82	39.8

[a] n.a. means not available.

in order to give a more accurate fit to the experimental results and n can be described as a degree of surface roughness and non-homogeneity. The shape of the impedance curves for blank (HCl alone) and that for all compounds features similarly a depressed semicircle, which indicates that the corrosion was mainly controlled by charge transfer. We thus illustrated their R_{ct} values which may reflect the solidness of the molecular film formed by the compound (if any) at the metal–solution interface in Figure 2 for a clearer comparison.[2–5,29–31]

The triazolyl glycolipid derivatives that feature relatively short lipid chains of 5C (**1**, **10**, **19**), 7C (**2**, **11**, **20**), and 9C (**3**, **12**, **21**) possess low R_{ct} values comparable to that of the blank, and poor inhibitive efficiencies ranging from 15% to 39%. In contrast, their analogues with prolonged lipid chains showed both slightly increased R_{ct} and η values. The C1- and C6-triazolyl glucolipid derivatives **4–9** and **12–18** bearing alkyl chains of 12C–18C have similar inhibitive efficiencies of around 45%. For the C6-triazolyl galactolipid analogues **22–27**, compound **23** with a 13C-alkyl chain exhibited the best efficiency (51%), whereas the η values of its counterparts **24–27** bearing further prolonged lipid chains lowered modestly.

Although it could seemingly be deduced that by coupling longer lipid chains of >12C with the sugar moiety via Cue-AAC, the resulting surface protective ability of the triazolyl glycolipids can be increased, there are yet no obvious structure–activity relationships (SARs) available among the three series. Neither the substitution position of the triazolyl lipid on the sugar scaffold (series 1 vs series 2) nor the C4-epimeric identity between glucose and galactose (series 2 vs series 3) is influential to their corrosion inhibitive potency.

Since our previously synthesized triazolyl monosaccharide–lipid conjugates failed to exhibit acceptable inhibitive potency against HCl corrosion for mild steel, we attempted to further prepare some disaccharide–lipid hybrids via Cue-AAC for evaluating whether the enlargement of the sugar moiety would bring on positive impact. As shown in Scheme 1, a known azido peracetyl

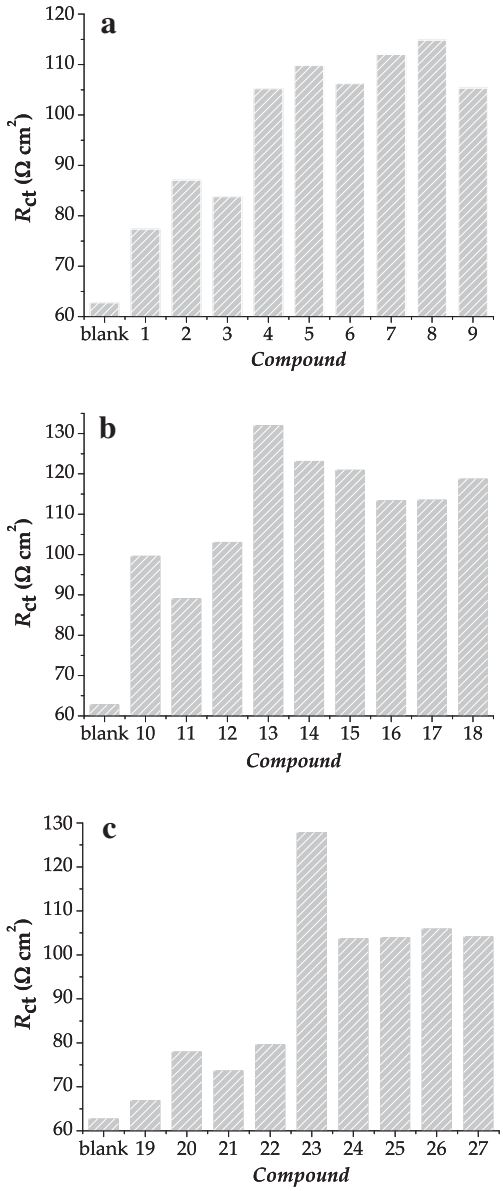

Figure 2. Collected R_{ct} values of mild steel in the absence (blank) and presence of compounds (a) **1**–**9**; (b) **10**–**18**; (c) **19**–**27**.

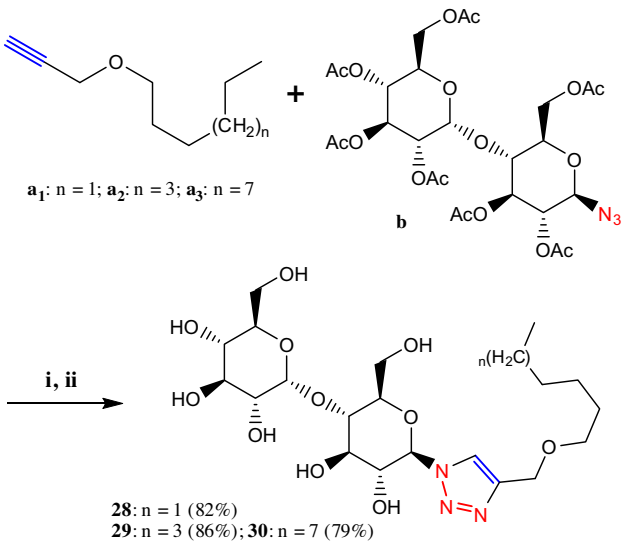

Scheme 1. Reagents and conditions: (i) $CuSO_4{\cdot}5H_2O$, Na ascorbate, CH_2Cl_2/H_2O; (ii) $MeOH/Et_3N/H_2O$.

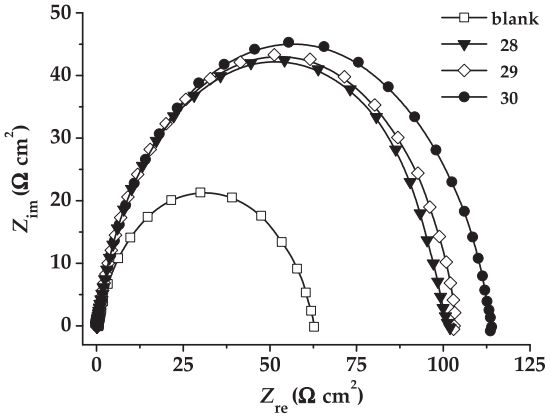

Figure 3. Nyquist plots of mild steel in 1 M HCl in the absence (blank) and presence of 10^{-3} M triazolyl maltose–lipid conjugates.

Table 2
EIS parameters for mild steel in 1 M HCl without (blank) and with compounds **28**–**30**

Compd	R_s (Ω cm^2)	R_{ct} (Ω cm^2)	CPE (μF cm^{-2})	n	η (%)
Blank	4.19	62.72	295.7	0.80	n.a.[a]
28	8.23	102.5	112.1	0.83	38.8
29	6.83	103.2	117.1	0.84	39.2
30	4.48	115.2	97.71	0.83	45.6

[a] n.a. means not available.

maltose **b**[32] and three propargyl fatty alcohols bearing alkyl chains of 6C ($\mathbf{a_1}$), 8C ($\mathbf{a_2}$), and 12C ($\mathbf{a_3}$), respectively, were used for the Cue-AAC. Under the action of Na ascorbate and $CuSO_4{\cdot}5H_2O$, the desired 1,4-disubstituted triazolyl conjugates were obtained as the unique products which were directly subject to deacetylation in $MeOH/Et_3N/H_2O$ by stirring over night. The desired triazole-connected maltose–lipid hybrids **28**–**30** were acquired in high yields of 80–86%.

The electrochemical process of mild steels in 1 M HCl in the presence of these compounds (10^{-3} M) was then evaluated via EIS. The resulting Nyquist plots are shown in Figure 3 and the EIS parameters obtained from the same circuit model are listed in Table 2. The capacitive curves of **28**–**30** displayed similar shape to those of their monosaccharide counterparts (Fig. S-1), indicating that the corrosion was likewise controlled by charge transfer.

However, as depicted by their unfavorable R_{ct} and η values (around 40%, Table 2) similar to those afforded by series 1–3 (Table 1), the triazolyl maltolipid derivatives prepared did not exhibit markedly enhanced inhibitive potency with respect to their glucoand galactolipid analogues. This demonstrates that enlargement of the sugar moiety does not improve the surface adsorptive ability of the triazolyl glycolipid derivatives.

Subsequently, we tended to introduce an additional functional group to a monosaccharide-based glycolipid scaffold via Cue-AAC in order to investigate whether such a structural modification would be effective. As heteroatom-rich compounds are known as preferred corrosion inhibitors due to their possession of lone pairs to coordinate with metals that have available empty d-orbital, we chose to introduce *p*-amino benzenesulfonamide (BSA) **c** that contains simultaneously O, N, and S atoms, and a benzene ring that may provide supplementary interactions with the metal surface, to a known glycolipid derivative $\mathbf{e_1}$ (Scheme 2).[24] Moreover, **c**

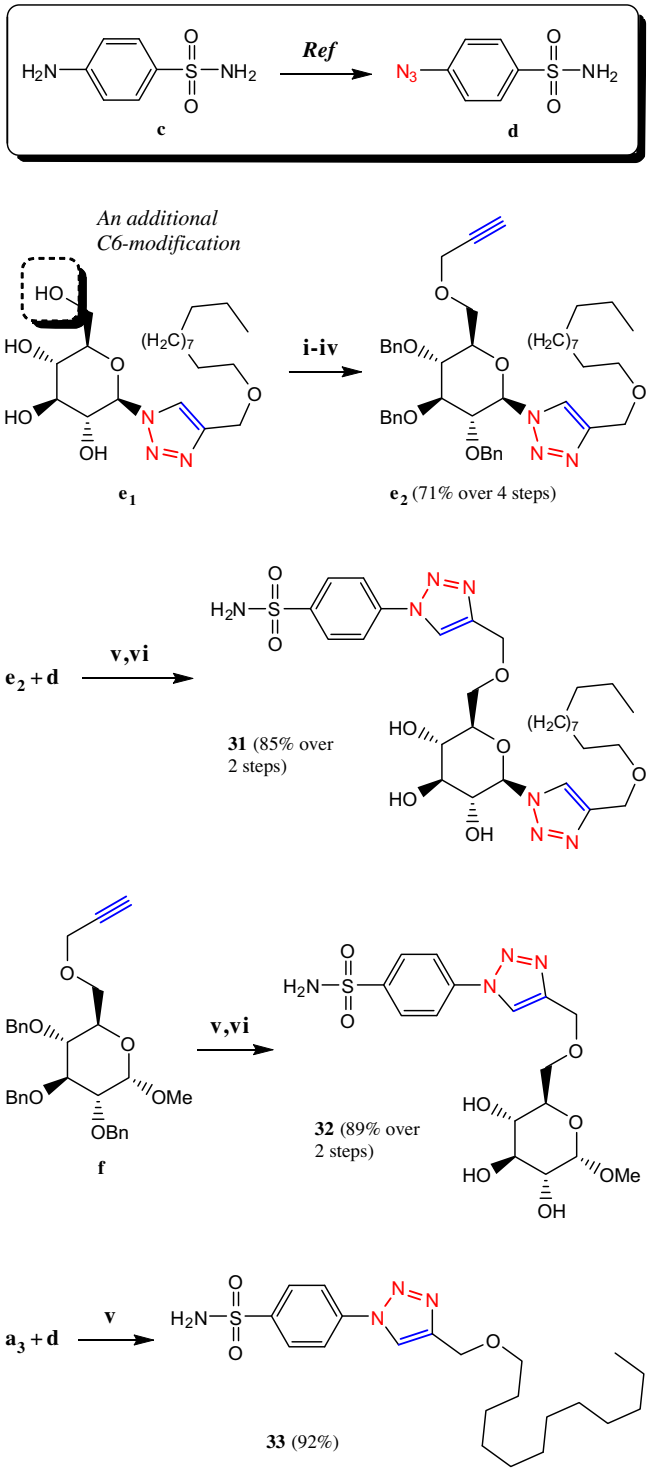

Scheme 2. Reagents and conditions: (i) TBDMSCl, DMAP, pyridine; (ii) NaH, BnBr, DMF; (iii) AcCl, MeOH; (iv) NaH, propargyl bromide, DMF; (v) $CuSO_4{\cdot}5H_2O$, Na ascorbate, CH_2Cl_2/H_2O/acetone; (vi) $PdCl_2/H_2$, MeOH/CH_2Cl_2.

frequently occurs in many drug entities, demonstrating its safety to human body.

As shown in Scheme 2, according to a literature method, *p*-azido BSA **d** was acquired.[33] A four-step sequence involving C6-silylation with TBDMSCl, O-benzylation with BnBr and NaH, C6-desilylation with AcCl, and then O-propargylation with propargyl bromide gave the C6-propargylated 1-triazolyl glycolipid $\mathbf{e_2}$ in 71% yield. Subsequent Cue-AAC of **d** with $\mathbf{e_2}$ led to a unique product which was directly subject to a debenzylation under the action of $PdCl_2/H_2$, affording the desired bis-triazolyl conjugate **31** with both a lipid chain and a BSA group attached on the sugar scaffold in 85% yield. For study of the SAR, compound **32** with solely a triazolyl BSA group on the C6-position of a methyl O-glucoside was synthesized by Cue-AAC of the known 6-*O*-propargyl methyl O-glucoside **f**[34] with the azide **d**, and then debenzylation with $PdCl_2/H_2$ in a two-step yield of 89%, while triazole-linked BSA–lipid conjugate **33** was synthesized via Cue-AAC of the propargyl lipid $\mathbf{a_3}$ with **d** in a high yield of 92%. The EIS of the prepared compounds was sequentially performed and the corresponding parameters were calculated through the same circuit model (Fig. 7).

We first observe that **c** alone displayed very weak inhibitive effect in HCl for mild steel (Fig. 4 and Table 3). However, to our delight, the bis-triazole conjugate **31** eventually exhibited favorable potency against the corrosion.

As shown in both Figure 4 and Table 3, the presence of bis-triazole **31** in 1 M HCl resulted in a significantly improved R_{ct} ($\eta = 87.3\%$) for mild steel in contrast with **13** and **30**, two mono-triazolyl analogues that exhibited the best potencies among the former glycolipid series. In order to evaluate whether the triazolyl BSA fragment functions dominantly in the context of the surface adsorption of **31**, the corrosion inhibitive profile of the mono-triazolyl BSA–methyl O-glucoside conjugate **32** and that of the triazolyl BSA–lipid conjugate **33** were also characterized via EIS (Fig. 4). As shown in Table 3, the inhibitive potency of **32** is as weak as those of the former mono-triazolyl lipid–sugar conjugates ($\eta = 40\%$) whereas that of **33** appeared to be only slightly better ($\eta = 65\%$). This clearly demonstrates that the additional Cue-AAC modification performed in fabricating the bis-triazolyl derivative based on a sugar scaffold is necessary for obtaining the adequate inhibitive efficiency against HCl corrosion.

Potentiodynamic polarization was then conducted under various concentrations of **31** for elaboration of its potential inhibitive mechanism and the resulting polarization curves are shown in Fig. 5. Polarization parameters including corrosion potential (E_{corr}), anodic (β_a) and cathodic (β_c) *Tafel* slopes and corrosion current density (i_{corr}), and the calculated surface coverage rate (θ) and inhibition efficiency (η) values are given in Table 4. Upon increase of the inhibitor in the solution, both β_a and β_c values varied accordingly and the i_{corr} values decreased prominently. This means that both the anodic metal dissolution of iron and the cathodic hydrogen evolution reaction were inhibited by **31**. Moreover, the η value (88.7%, Table 4) at the highest inhibitor concentration (10^{-3} M) obtained from *Tafel* extrapolation is in a good agreement with that obtained by EIS (87.3%, Table 3). The corrosion potential of mild

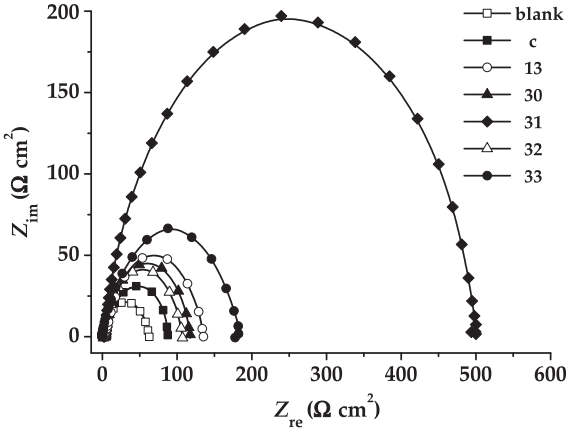

Figure 4. Nyquist plots of mild steel in 1 M HCl in the absence (blank) and presence of 10^{-3} M compounds.

Table 3
EIS parameters for mild steel in 1 M HCl without (blank) and with compounds **c**, **13** and **30–33**

Compd	R_s (Ω cm^2)	R_{ct} (Ω cm^2)	CPE (μF cm^{-2})	n	η (%)
Blank	4.19	62.72	295.7	0.80	n.a.[a]
c	5.24	86.92	250.9	0.79	27.8
13	10.76	131.9	121.6	0.80	52.4
30	4.48	115.2	97.71	0.83	45.6
31	3.90	494.7	55.03	0.83	87.3
32	7.38	104.5	122.9	0.82	40.0
33	7.08	177.9	159.9	0.80	64.7

[a] n.a. means not available.

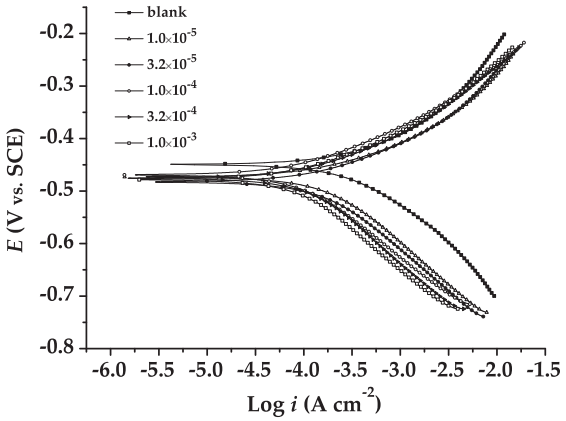

Figure 5. Polarization curves of mild steel in 1 M HCl in the absence (blank) and presence of various concentrations of compound **31**.

steel in the presence of the inhibitor shifted by 2–18 mV as regards that of the blank, which suggests that **31** behaves as a mixed-type corrosion inhibitor for mild steel by first adsorbing on the metal surface and then blocking the reaction sites of the metal surface without affecting the anodic and cathodic reactions.[29]

Adsorption isotherm calculations were sequentially performed to further assess the inhibitive mechanism of **31** by tentatively fitting the above-obtained θ values (Table 4) at various concentrations (C) to Temkin, Frumkin, Freundluich, and Langmuir isotherm models, respectively. The best correlation between the experimental results and isotherm functions was obtained using the Langmuir adsorption isotherm interpreted by the following equation: $C/\theta = 1/K_{ads} + C$ (where K_{ads} is the equilibrium constant of the adsorption process). Plotting of C versus C/θ resulted in a linear correlation (Fig. 6) and the standard free energy of adsorption (G^0_{ads}) was estimated by the following equation: $K_{ads} = (1/55.5)\exp(-\Delta G^0_{ads}/RT)$ (where 55.5 is the molar concentration of water in the solution expressed in the molarity unit M). As shown in Table 5, the ΔG^0_{ads} value (−39.7) obtained indicates that the adsorption process of **31** to the surface is spontaneous and the interaction of the adsorbed layer with the steel surface is stable.

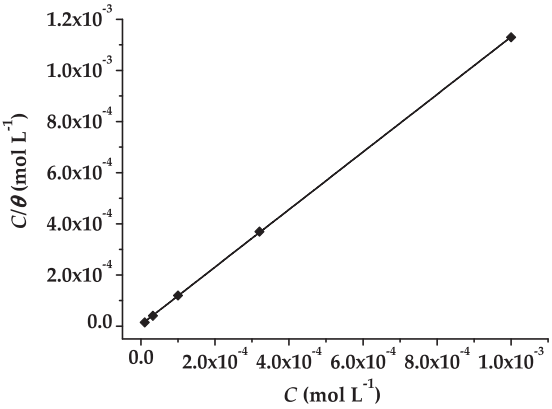

Figure 6. Langmuir isotherm of **31** adsorbing onto the mild steel surface in 1 M HCl at 298 K.

Table 5
The calculated K_{ads} and ΔG^0_{ads} values for mild steel in 1 M HCl containing inhibitor **31** at 298 K

Compd	T (K)	Slope	K_{ads} (M^{-1})	ΔG^0_{ads} (kJ mol^{-1})
31	298	1.12	166881.9	−39.7

Meanwhile, it can be deduced that this inhibitor adopts both electrostatic-adsorption and chemo-adsorption on the mild steel surface in 1 M HCl, whereas the latter is privileged.[30]

3. Conclusion

To summarize, series of our previously prepared triazolyl glycolipid derivatives were manifested not to be good corrosion inhibitors for mild steel in 1 M HCl via EIS, whereas the successively synthesized triazolyl disaccharide–lipid conjugates via Cue-AAC also displayed weak potency for mild steel protection. This first implies that the structural variations such as the change in the substitution position of the triazolyl lipid on the sugar moiety, the prolongation of the lipid chain and the enlargement of the sugar ring do not enhance positively the corrosion inhibitive competency of triazolyl glycolipid derivatives. A subsequent stepwise Cue-AAC strategy by grafting an additional heteroatom-rich BSA group to a 'pre-clicked' glucolipid derivative led to, however, an admirable inhibitor **31** with remarkably improved protective potency for mild steel in HCl. Moreover, its analogues **32** with solely a triazolyl BSA substituent on a methyl O-glucoside and the mono-triazolyl BSA–lipid conjugate **33** exhibited markedly decreased potency, indicating that the triazolyl lipid and BSA functionalities together might exert a synergistic effect in their surface adsorptive process. Polarization and isotherm calculations eventually elaborated that **31** is a mixed-type inhibitor and adopts mainly chemo-adsorption toward the metal surface. This study would thus offer collectively new

Table 4
Polarization parameters for mild steel in 1 M HCl without (blank) and with various concentrations of compound **31**

31 (M)	E_{corr} (mV)	i_{corr} (μA cm^2)	β_a (mV dec^{-1})	$-\beta_c$ (mV dec^{-1})	θ	η (%)
Blank	−470.7	654.2	191.9	194.4	n.a[a]	n.a.
1.0×10^{-5}	−488.2	203.9	106.7	157.9	0.69	68.8
3.2×10^{-5}	−474.7	140.2	77.78	159.5	0.79	78.6
1.0×10^{-4}	−478.6	106.9	101.8	151.9	0.84	83.7
3.2×10^{-4}	−472.2	88.44	77.91	159.3	0.86	86.5
1.0×10^{-3}	−472.8	74.18	78.59	158.4	0.89	88.7

[a] n.a. means not available.

insights into the future design and construction of triazolyl glycolipid derivatives as potential corrosion inhibitors.

4. Experimental section

4.1. Synthesis

Solvents were purified by standard procedures. Petroleum ether (PE) used refers to the fraction boiling in the range 60–90 °C. ^{1}H and ^{13}C NMR spectra were recorded on a Bruker AM-400 spectrometer in $CDCl_3$, D_2O or CD_3OD solutions using TMS as the internal standard (chemical shifts in parts per million). Standard abbreviations are used to describe the signal multiplicity. All reactions were monitored by TLC (Yantai Marine Chemical Co. Ltd, China). High resolution mass spectra (HRMS) were recorded on a Waters LCT Premier XE spectrometer using standard conditions (ESI, 70 eV). Analytical HPLC was measured using Agilent 1100 Series equipment.

4.1.1. General procedure for the synthesis of compounds 28–30

To a well-stirred biphasic solution of the per-O-acetylated glycosyl azide (1 equiv) and the alkynyl ether (2 equiv) in CH_2Cl_2 (8–10 mL) and H_2O (6 mL), were added $CuSO_4{\cdot}5H_2O$ (1.5 equiv) and sodium ascorbate (2.5 equiv), and this mixture was stirred at rt for 6 h. The resulting mixture was diluted with CH_2Cl_2 and then washed with brine. The combined organic layer was dried over $MgSO_4$ and then concentrated under reduced pressure to give a crude residue which was directly dissolved in MeOH/Et_3N/H_2O (8:1:1, V/V/V) and stirred overnight at rt. The resulting solution was concentrated to dryness to give a thick syrup which was purified by column chromatography.

4.1.1.1. (1-β-D-Maltosyl-1*H*-1,2,3-triazol-4-yl)methyl *n*-hexyl ether (28). From **b** (217.4 mg, 0.329 mmol) and $\mathbf{a_1}$ (92.2 mg, 0.66 mmol), column chromatography (CH_2Cl_2–EtOH, 3:1→3:2) afforded **28** as a white solid (137.3 mg, 82.2%). TLC: R_f = 0.60 (CH_2Cl_2–MeOH, 1:1). ^{1}H NMR (400 MHz, D_2O) δ 8.28 (s, 1H), 5.80 (d, J = 8.5 Hz, 1H), 5.51 (d, J = 3.8 Hz, 1H), 4.70 (s, 2H), 4.09–4.00 (m, 2H), 3.95 (d, J = 12.0 Hz, 1H), 3.92–3.87 (m, 3H), 3.86 (d, J = 13.4 Hz, 1H), 3.82–3.70 (m, 3H), 3.63 (dd, J = 10.0, 4.0 Hz, 1H), 3.61 (t, J = 6.8 Hz, 2H), 3.46 (t, J = 9.4 Hz, 1H), 1.59 (m, 2H), 1.36–1.23 (br m, 6H), 0.86 (t, J = 6.8 Hz, 3H); ^{13}C NMR (100 MHz, D_2O) δ 144.5, 123.9, 99.9, 87.3, 77.5, 76.4, 76.2, 72.9, 72.8, 72.2, 71.8, 70.7, 69.3, 63.0, 60.5, 60.4, 31.4, 29.0, 25.3, 22.3, 13.5; HR-ESI-MS m/z: calcd for $C_{21}H_{37}N_3O_{11}$ + H 508.2506, found 508.2504.

4.1.1.2. (1-β-D-Maltosyl-1*H*-1,2,3-triazol-4-yl)methyl *n*-octyl ether (29). From **b** (203.9 mg, 0.31 mmol) and $\mathbf{a_2}$ (103.7 mg, 0.62 mmol), column chromatography (CH_2Cl_2–EtOH, 3:1→3:2) afforded **29** as a white solid (141.2 mg, 85.6%). TLC: R_f = 0.68 (CH_2Cl_2–MeOH, 1:1). ^{1}H NMR (400 MHz, D_2O) δ 8.15 (s, 1H), 5.71 (d, J = 7.7 Hz, 1H), 5.45 (d, J = 3.0 Hz, 1H), 4.54 (s, 2H), 4.00 (m, 2H), 3.91–3.81 (m, 4H), 3.75 (m, 4H), 3.62 (dd, J = 10.0, 3.1 Hz, 1H), 3.53–3.42 (m, 3H), 1.57 (br s, 2H), 1.30 (br s, 10H), 0.89 (t, J = 6.0 Hz, 3H); ^{13}C NMR (100 MHz, D_2O + CD_3OH) δ 144.6, 123.9, 100.2, 87.5, 77.7, 76.6, 73.1, 72.9, 72.3, 72.0, 70.9, 69.4, 63.4, 60.7, 60.6, 32.0, 29.6, 29.4, 26.1, 22.8, 14.0; HR-ESI-MS m/z: calcd for $C_{23}H_{41}N_3O_{11}$ + H 536.2819, found 536.2820.

4.1.1.3. (1-β-D-Maltosyl-1*H*-1,2,3-triazol-4-yl)methyl *n*-dodecyl ether (30). From **b** (177.5 mg, 0.27 mmol) and $\mathbf{a_3}$ (120.4 mg, 0.54 mmol), column chromatography (CH_2Cl_2–EtOH, 3:1→2:1) afforded **30** as a white solid (124.6 mg, 78.6%). TLC: R_f = 0.69 (CH_2Cl_2–MeOH, 1:1). ^{1}H NMR (400 MHz, CD_3OD) δ 8.15 (s, 1H), 5.62 (d, J = 9.1 Hz, 1H), 5.23 (d, J = 3.7 Hz, 1H), 4.57 (s, 2H), 3.94 (t, J = 9.1 Hz, 1H), 3.87 (dd, J = 14.5, 2.2 Hz, 2H), 3.82 (m, 2H), 3.75 (t, J = 9.1 Hz, 1H), 3.71 (m, 1H), 3.69–3.60 (m, 3H), 3.49 (t, J = 6.6 Hz, 2H), 3.47 (dd, J = 8.8, 3.7 Hz, 1H), 3.27 (t, J = 9.3 Hz, 1H), 1.56 (m, 2H), 1.26 (br s, 18H), 0.87 (t, J = 6.8 Hz, 3H); ^{13}C NMR (100 MHz, $CDCl_3$ + CD_3OH) δ 144.6, 123.3, 100.9, 87.5, 77.7, 76.5, 73.5, 72.9, 72.2, 71.1, 69.5, 63.6, 60.9, 60.6, 57.8, 31.8, 29.6, 29.5, 29.5, 29.4, 29.3, 29.2, 25.9, 22.5, 17.9, 13.9; HR-ESI-MS m/z: calcd for $C_{27}H_{49}N_3O_{11}$ + H 592.3445, found 592.3441.

4.1.2. Synthesis of [1-(2,3,4-Tri-*O*-benzyl-6-*O*-propargyl-β-D-glucopyranosyl)-1*H*-1,2,3-triazol-4-yl]methyl *n*-dodecyl ether ($\mathbf{e_2}$)

To a well-stirred solution of $\mathbf{e_1}$ (400 mg, 0.93 mmol) in pyridine (7 mL) at 0 °C were added TBDMSCl (196.4 mg, 1.30 mmol) and DMAP (45.5 mg, 0.37 mmol). The mixture was then allowed to reach rt and stirred for 6 h. The resulting mixture was concentrated under reduced pressure and the residue was diluted with CH_2Cl_2 and washed successively with 1 N HCl and 5% aq $NaHCO_3$. The combined organic layer was dried over $MgSO_4$ and concentrated under reduced pressure to give a crude product which was dissolved in DMF (8 mL). BnBr (443.8 μL, 3.72 mmol) was added and the resulting solution was cooled to 0 °C, followed by addition of 60% NaH (148.8 mg, 3.72 mmol) in 3 batches. After stirring at rt for 2 h, the reaction was quenched with MeOH (2 mL) and the mixture was concentrated in vacuum. The residue was diluted with EtOAc and washed successively with 1 N HCl and brine. The organic layer was combined, dried over $MgSO_4$ and concentrated under reduced pressure. The resulting crude residue was dissolved in MeOH (12 mL) and cooled to 0 °C. AcCl (329.2 μL, 4.66 mmol) was added dropwise and the mixture was stirred at rt for 1 h. The resulting mixture was concentrated under reduced pressure and the resulting residue was dissolved directly in DMF (8 mL), followed by addition of propargyl bromide (109.3 μL, 1.40 mmol). The resulting mixture was cooled to 0 °C and 60% NaH (56.0 mg, 1.40 mmol) was added. After stirring at rt for 6 h, H_2O (8 mL) was added and the mixture was concentrated under reduced pressure. The resulting residue was diluted with EtOAc and washed with brine. The combined organic layers were dried over $MgSO_4$, concentrated under reduced pressure and eventually purified by column chromatography (petroleum ether–EtOAc, 6:1→2:1) to give $\mathbf{e_2}$ (492.3 mg, 71.7% over 4 steps) as a white crystalline solid. TLC: R_f = 0.60 (petroleum ether–EtOAc, 2:1). ^{1}H NMR (400 MHz, $CDCl_3$) δ 7.58 (s, 1H), 7.30–7.20 (m, 10H), 7.16–7.10 (m, 3H), 6.88 (dd, J = 6.6, 2.8 Hz, 2H), 5.51 (d, J = 9.1 Hz, 1H), 4.86 (s, 2H), 4.83 (d, J = 10.8 Hz, 1H), 4.68 (d, J = 10.8 Hz, 1H), 4.55 (dd, J = 15.2, 12.8 Hz, 2H), 4.41 (d, J = 10.5 Hz, 1H), 4.13 (dd, J = 15.9, 2.4 Hz, 1H), 4.03 (dd, J = 15.9, 2.3 Hz, 1H), 3.98 (dd, J = 16.0, 9.7 Hz, 2H), 3.81–3.71 (m, 3H), 3.67 (dd, J = 10.9, 1.5 Hz, 1H), 3.65–3.60 (m, 1H), 3.42 (t, J = 6.7 Hz, 2H), 2.31 (t, J = 2.3 Hz, 1H), 1.50 (m, 2H), 1.17 (br s, 18H), 0.81 (t, J = 6.8 Hz, 3H).

4.1.3. Synthesis of 4-{4-[(4-*n*-Dodecyloxymethyl-1*H*-1,2,3-triazol-1-yl)β-D-glucopyranosd-6-yloxy]methyl-1*H*-1,2,3-triazol-1-yl} benzenesulfonamide (31)

To a well-stirred biphasic solution of $\mathbf{e_2}$ (106 mg, 0.14 mmol) and **d** (42.7 mg, 0.22 mmol) in CH_2Cl_2/H_2O/acetone (10:5:1, V/V/V) were added $CuSO_4{\cdot}5H_2O$ (107.6 mg, 0.43 mmol) and sodium ascorbate (170.7 mg, 0.86 mmol), and the mixture was stirred at 30 °C for 6 h. The resulting mixture was then diluted with CH_2Cl_2 and washed with saturated aq ethylene diamine tetraacetic acid (EDTA) and brine. The combined organic layer was dried over $MgSO_4$ and concentrated under reduced pressure to give a crude residue. This was then dissolved in MeOH/CH_2Cl_2 (2:1, V/V) and $PdCl_2$ (10 mg, 0.0564 mmol) was added. The mixture was stirred vigorously under hydrogen atmosphere at 35 °C for 1 h. The resulting mixture was then filtered and concentrated under reduced pressure. The resulting crude residue was purified by column chro-

matography (CH_2Cl_2–EtOH, 10:1→4:1) to give **31** (81.7 mg, 85.2%) as a white solid. TLC: R_f = 0.57 (CH_2Cl_2–MeOH, 4:1). ^{1}H NMR (400 MHz, CD_3OD) δ 8.50 (s, 1H), 8.12 (s, 1H), 8.05 (d, J = 8.8 Hz, 2H), 7.95 (d, J = 8.7 Hz, 2H), 5.60 (d, J = 9.2 Hz, 1H), 4.69 (d, J = 2.4 Hz, 2H), 4.54 (s, 2H), 3.96–3.88 (m, 2H), 3.81 (dd, J = 11.1, 5.3 Hz, 1H), 3.73 (dd, J = 8.1, 5.1 Hz, 1H), 3.60–3.52 (m, 2H), 3.47 (t, J = 6.6 Hz, 2H), 1.53 (m, 2H), 1.24 (br s, 18H), 0.86 (t, J = 6.8 Hz, 3H); ^{13}C NMR (100 MHz, CD_3OD) δ 145.1, 140.5, 129.1, 124.4, 123.3, 121.5, 89.5, 79.9, 79.6, 79.2, 78.9, 78.4, 73.8, 71.9, 70.8, 70.7, 65.3, 64.6, 33.1, 30.8, 30.8, 30.8, 30.7, 30.6, 30.5, 27.2, 23.8, 14.6; HR-ESI-MS m/z: calcd for $C_{30}H_{47}N_7O_8S$ + H 666.3285, found 666.3290; HPLC (t_R = 4.5 min over 20 min of 100% methanol, purity 100%).

4.1.4. Synthesis of 4-[4-(Methyl α-D-glucopyranosid-6-yloxy)methyl-1*H*-1,2,3-triazol-1-yl] benzenesulfonamide (32)

To a well-stirred biphasic solution of **f** (343 mg, 0.68 mmol) and **d** (175.8 mg, 0.89 mmol) in CH_2Cl_2/H_2O/Acetone (3:1:1, V/V/V) were added $CuSO_4{\cdot}5H_2O$ (221.5 mg, 0.89 mmol) and sodium ascorbate (351.5 mg, 1.77 mmol). After stirring at rt for 6 h, the resulting mixture was diluted with CH_2Cl_2 (12 mL) and then washed with aq EDTA and brine. The combined organic layer was dried over $MgSO_4$ and then concentrated under reduced pressure to give a crude residue. This was then dissolved in MeOH/CH_2Cl_2 (6:1, V/V) and $PdCl_2$ (30.0 mg, 0.169 mmol) was added. The mixture was stirred vigorously under hydrogen atmosphere at 35 °C for 40 min and the resulting mixture was filtered and concentrated under reduced pressure. The crude residue was purified by column chromatography (CH_2Cl_2–MeOH, 8:1→3:1) to give **32** (261.9 mg, 89.1%) as a white solid. TLC: R_f = 0.27 (CH_2Cl_2–MeOH, 4:1). ^{1}H NMR (400 MHz, CD_3OD) δ 8.60 (s, 1H), 8.05 (d, J = 8.4 Hz, 2H), 7.99 (d, J = 8.4 Hz, 2H), 7.79 (br s, 2H), 4.74 (s, 2H), 4.66 (d, J = 3.4 Hz, 1H), 3.82 (d, J = 9.8 Hz, 1H), 3.77 (dd, J = 10.9, 4.6 Hz, 1H), 3.69–3.64 (m, 1H), 3.62 (d, J = 9.3 Hz, 1H), 3.43 (d, J = 3.4 Hz, 1H), 3.40 (d, J = 3.3 Hz, 1H), 3.36 (s, 3H); ^{13}C NMR (100 MHz, CD_3OD) δ 147.3, 145.1, 140.6, 129.2, 123.5, 121.7, 101.2, 79.7, 79.5, 79.3, 79.0, 75.1, 73.4, 72.4, 71.5, 71.0, 65.4, 56.0; HR-ESI-MS m/z: calcd for $C_{16}H_{22}N_4O_8S$ + H 431.1237, found 431.1238; HPLC (t_R = 3.9 min over 20 min of 100% methanol, purity 94.3%).

4.1.5. Synthesis of 4-(4-*n*-dodecyloxymethyl-1*H*-1,2,3-triazol-1-yl) benzenesulfonamide (33)

To a well-stirred biphasic solution of $\mathbf{a_3}$ (230.9 mg, 1.03 mmol) and **d** (136 mg, 0.69 mmol) in CH_2Cl_2/acetone/H_2O (3:3:2, V/V/V) were added $CuSO_4{\cdot}5H_2O$ (222.7 mg, 0.89 mmol) and sodium ascorbate (312.7 mg, 1.58 mmol). After stirring at rt for 12 h, the resulting mixture was condensed under reduced pressure to half volume, diluted with CH_2Cl_2 and washed with aq EDTA and brine. The combined organic layer was dried over $MgSO_4$ and then concentrated under reduced pressure to give a light yellow solid. Subsequent recrystallization (petroleum ether/CH_2Cl_2/MeOH, 15:5:1) afforded **33** as a white solid (267.3 mg, 92.2%). TLC: R_f = 0.51 (petroleum ether–EtOAc, 1:1). ^{1}H NMR (400 MHz, $CDCl_3$ + CD_3OD) δ 8.55 (s, 1H), 8.09 (d, J = 8.8 Hz, 2H), 8.03 (d, J = 8.8 Hz, 2H), 4.68 (s, 2H), 3.57 (t, J = 6.6 Hz, 2H), 1.62 (m, 2H), 1.26 (s, 18H), 0.88 (t, J = 6.7 Hz, 3H); ^{13}C NMR (100 MHz, $CDCl_3$ + CD_3OD + DMSO-d_6) δ 147.1, 144.6, 140.1, 128.7, 122.6, 121.2, 71.6, 64.4, 32.6, 30.4, 30.3, 30.3, 30.1, 30.0, 26.8, 23.4, 14.5; HR-ESI-MS m/z: calcd for $C_{21}H_{34}N_4O_3S$ + H 423.2430, found 423.2429; HPLC (t_R = 6.6 min over 20 min of 50% methanol/acetonitrile, purity 94.2%).

4.2. Electrochemistry

The mild steel having a composition (wt.%) of 0.20% C, 0.16% Si, 0.35% Mn, 0.05% P, 0.01 S and the balance Fe was used for electrochemical study in 1 M HCl solution (freshly prepared in H_2O/EtOH = 1:1, V/V). The electrochemical experiments were carried out using a conventional three-electrode cell assembly at rt. Mild steel strips with a 1.0 cm^2 exposed surface area were used as working electrode, platinum foil was used as the counter electrode, and a saturated calomel electrode (SCE) was used as the reference electrode. The potentiodynamic polarization curves were obtained from −250 mV_{SCE} to +250 mV_{SCE} (vs open circuit potential [OCP]) with a sweep rate of 0.5 mV/s on a CHI660C apparatus. EIS measurements were carried out in 100 kHz to 10 mHz frequency range at the steady OCP disturbed with an amplitude of 10 mV on a ZAHNER apparatus. The raw electrochemical data were collected and analyzed by the electrochemical software ZSimpWin. The EIS parameters were calculated using the following circuit model:

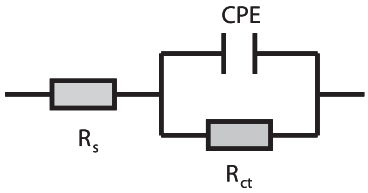

Figure 7. Electric circuit model for the EIS plots.

The inhibition efficiency (η, %) was calculated by η (%) = $(R_{ct} - R_{ct0})/R_{ct} \times 100 = (i_{corr0} - i_{corr})/i_{corr0} \times 100$, where R_{ct} and R_{ct0} are the charge transfer resistances in the presence and absence of the inhibitors and i_{corr} and i_{corr0} are the polarization current densities in the presence and absence of the inhibitors, respectively.

Acknowledgements

Generous funding is provided by the National Natural Science Foundation of China (Grant 21176076), Shanghai Science and Technology Community (Grant 10410702700) and the Fundamental Research Funds for the Central Universities (No. WK1013002). X.-P. He is also supported by China Postdoctoral Science Foundation (No. 2011M500069) and he warmly thanks the French Embassy in PR China for a co-tutored doctoral program and his French advisor Professor Juan Xie at ENS Cachan.

Supplementary data

Supplementary data associated with this article can be found, in the online version, at http://dx.doi.org/10.1016/j.carres.2012.03.006.

References

1. Sinko, J. *Prog. Org. Coat.* **2001**, *42*, 267–282.
2. Raja, P. B.; Sethuraman, M. G. *Mater. Lett.* **2008**, *62*, 113–116.
3. Khald, K. F. *Corros. Sci.* **2010**, *52*, 3225–3234.
4. Gece, G.; Bilgiç, S. *Corros. Sci.* **2010**, *52*, 3435–3443.
5. Mohammed, A. A.; Khaled, K. F.; Mohsen, Q.; Arida, H. A. *Corros. Sci.* **2010**, *52*, 1684–1695.
6. Kolb, H. C.; Finn, M. G.; Sharpless, K. B. *Angew. Chem., Int. Ed.* **2001**, *40*, 2004–2021.
7. Tornøe, C. W.; Christensen, C.; Meldal, M. *J. Org. Chem.* **2002**, *67*, 3057–3064.
8. Rostovtsev, V. V.; Green, L. G.; Fokin, V. V.; Sharpless, K. B. *Angew. Chem., Int. Ed.* **2002**, *41*, 2596–2599.
9. Wang, Q.; Hawker, C. *Chem. Asian J.* **2011**, *6*, 2568–2569.
10. Aragão-Leoneti, V.; Campo, V. L.; Gomes, A. S.; Field, R. A.; Carvalho, I. *Tetrahedron* **2010**, *49*, 9475–9492.
11. Chen, Y.-B.; Wang, Y.-J.; Lin, Y.-J.; Hu, C.-H.; Chen, S.-J.; Chir, J.-L.; Wu, A.-T. *Carbohydr. Res.* **2010**, *345*, 956–959.
12. Dedola, S.; Hughes, D. L.; Nepogodiev, S. A.; Rejzek, M.; Field, R. A. *Carbohydr. Res.* **2010**, *345*, 1123–1134.
13. Rajaganesh, R.; Jayakumar, J.; Sivaraj, C.; Raaman, N.; Das, T. M. *Carbohydr. Res.* **2010**, *345*, 1649–1657.
14. Kumar, K. K.; Kumar, R. M.; Subramanian, V.; Das, T. M. *Carbohydr. Res.* **2010**, *345*, 2297–2304.
15. Guillemineau, M.; Singh, S.; Grossutti, M.; Auzanneau, F.-I. *Carbohydr. Res.* **2010**, *345*, 2723–2730.

16. Fu, Q.; Liang, T.; Zhang, X.; Du, Y.; Guo, Z.; Liang, X. *Carbohydr. Res.* **2010**, *345*, 2690–2697.
17. Benoist, E.; Coulais, Y.; Almant, M.; Kovensky, J.; Moreau, V.; Lesur, D.; Artigau, M.; Picard, C.; Galaup, C.; Gouin, S. G. *Carbohydr. Res.* **2011**, *346*, 26–34.
18. Song, Z.; He, X.-P.; Li, C.; Gao, L.-X.; Wang, Z.-X.; Tang, Y.; Xie, J.; Li, J.; Chen, G.-R. *Carbohydr. Res.* **2011**, *346*, 140–145.
19. Anand, N.; Jaiswal, N.; Pandey, S. K.; Srivastava, A. K.; Tripathi, R. P. *Carbohydr. Res.* **2011**, *346*, 16–25.
20. Tran, D. N.; Blaszkiewicz, C.; Menuel, S.; Roucoux, A.; Philippot, K.; Hapiot, F.; Monflier, E. *Carbohydr. Res.* **2011**, *346*, 210–218.
21. Li, T.; Guo, L.; Zhang, Y.; Wang, J.; Li, Z.; Lin, L.; Zhang, Z.; Li, L.; Lin, J.; Zhao, W.; Li, J.; Wang, P. G. *Carbohydr. Res.* **2011**, *346*, 1083–1092.
22. Kumar, K. K.; Seenivasan, S. P.; Kumar, V.; Das, T. M. *Carbohydr. Res.* **2011**, *346*, 2084–2090.
23. Rajaganesh, R.; Ravinder, P.; Subramanian, V.; Das, T. M. *Carbohydr. Res.* **2011**, *346*, 2327–2336.
24. Paul, K. J.; Loganathan, D. *Tetrahedron Lett.* **2008**, *49*, 6356–6359.
25. Neto, V.; Granet, R.; Krausz, P. *Tetrahedron* **2010**, *66*, 4633–4646.
26. Song, S.-X.; Zhang, H.-L.; Kim, C.-G.; Sheng, L.; He, X.-P.; Long, Y.-T.; Li, J.; Chen, G.-R. *Tetrahedron* **2010**, *66*, 9974–9980.
27. Zhang, H.-L.; He, X.-P.; Sheng, L.; Yao, Y.; Zhang, W.; Shi, X.-X.; Li, J.; Chen, G.-R. *Mol. Divers.* **2011**, *15*, 889–900.
28. He, X.-P.; Xu, X.; Zhang, H.-L.; Chen, G.-R.; Xu, S.; Liu, H. *Carbohydr. Res.* **2011**, *346*, 1320–1326.
29. Bentiss, F.; Bouanis, M.; Mernari, B.; Traisnel, M.; Vezin, H.; Lagrenée, M. *Appl. Surf. Sci.* **2007**, *253*, 3696–3704.
30. Lebrini, M.; Lagrenée, M.; Vezin, H.; Traisel, M.; Bentiss, F. *Corros. Sci.* **2007**, *49*, 2254–2269.
31. Deng, Q.; Shi, H.-W.; Ding, N.-N.; Chen, B.-Q.; He, X.-P.; Liu, G.; Tang, Y.; Long, Y.-T.; Chen, G.-R. *Corros. Sci.* **2012**, *57*, 220–227.
32. Kumar, R.; Maulik, P. R.; Misra, A. K. *Glycoconjugate J.* **2008**, *25*, 595–602.
33. Das, J.; Patil, S. N.; Awasthi, R.; Narasimhulu, C. P.; Trehan, S. *Synthesis* **2005**, 1801–1806.
34. He, X.-P.; Li, C.; Jin, X.-P.; Song, Z.; Zhang, H.-L.; Zhu, C.-J.; Shen, Q.; Zhang, W.; Sheng, L.; Shi, X.-X.; Tang, Y.; Li, J.; Chen, G.-R.; Xie, J. *New J. Chem.* **2011**, *35*, 622–631.